10

The 't Hooft solution of 2d QCD

Two-dimensional quantum chromodynamics involves an $SU(N)$ symmetry group. We saw that models get simplified in the large N limit, and so we would like to examine the question of whether the large N limit QCD in two dimensions can be solved. This question was addressed by 't Hooft who showed that indeed QCD_2 in this limit is almost exactly soluble. The simplest Green's functions can be solved in closed forms and the meson spectrum can be extracted by a non-elaborate numerical computation.

This was derived by 't Hooft in his seminal paper [124], and it had many follow ups. In this chapter we consider only [56], which discusses the scattering properties of QCD in the large N model.

Recall the action of a two-dimensional QCD,

$$S_{QCD} = -\frac{1}{2}\mathrm{Tr}[F_{\mu\nu}F^{\mu\nu}] + \bar{\Psi}_i(i\not{D} - m_i)\Psi_i, \tag{10.1}$$

where the gauge fields are spanned by $N \times N$ Hermitian matrices T^A such that $A_\mu = A_\mu^A T^A$, $F_{\mu\nu} = \partial_\mu A_\nu - \partial_\nu A_\mu + i\frac{g}{\sqrt{N}}[A_\mu, A_\nu]$, the covariant derivative $D_\mu = \partial_\mu + i\frac{g}{\sqrt{N}}A_\mu$, the fermions Ψ are in the fundamental representation of the color group and $i = 1, \ldots, N_f$ indicates the flavor degrees of freedom. There is a sum over the flavor indices. Note that the gauge coupling was chosen to be $\frac{g}{\sqrt{N}}$, obviously to accommodate a large N approximation with g fixed.

It is convenient to impose the algebraic light-cone gauge. This gauge is advantageous at least for the following two reasons:

(i) The field strength F_{+-} becomes linear in the gauge potential,

$$A^+ = A_- = 0 \quad \Rightarrow \quad F_{+-} = -\partial_- A_+. \tag{10.2}$$

(ii) The theory after gauge fixing is still Lorentz invariant. This is obviously a property of two dimensions only.

In this gauge the Lagrangian of the system becomes,

$$\mathcal{L} = -\frac{1}{2}\mathrm{Tr}[(\partial_- A_+)^2] + \bar{\Psi}_k\left(i\not{\partial} - m_k - \frac{g}{\sqrt{N}}\gamma_- A_+\right)\Psi_k. \tag{10.3}$$

Recall that in the light-cone gauge there are no ghost fields.

The Feynman rules associated with this action in the so-called double line notation follow from Fig. 10.1, as explained below.

In the following we shall be taking one flavor, for simplicity.

https://doi.org/10.1017/9781009401654.011 Published online by Cambridge University Press

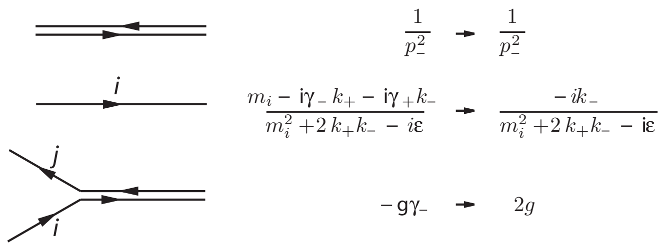

Fig. 10.1. The Feynman rules of QCD_2 in the light cone.

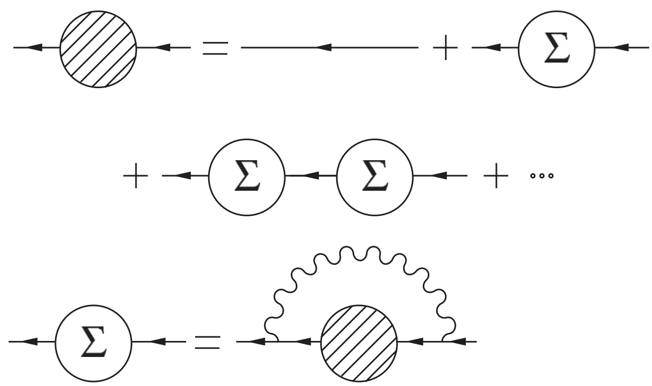

Fig. 10.2. The quark self-energy.

The light-cone gamma matrices obey the relations,

$$\gamma_-^2 = \gamma_+^2 = 0 \quad \{\gamma^+, \gamma^-\} = 2. \tag{10.4}$$

Since the vertex is proportional to γ_-, only that part of the propagator that is proportional to γ_+ can contribute. As a consequence we can eliminate all the γ dependence from the Feynman diagrams. Thus the double line, representing the gluon propagator, is $\frac{1}{p_-^2}$, the fermion line is $\frac{-ik_-}{m^2+2k_+k_- - i\epsilon}$, and the coupling is $2g$.

Note that for the gauge field propagator one makes use of the principal value such that,

$$D_{++}(p) = \mathcal{P}\left(\frac{1}{p_-^2}\right) \equiv \frac{1}{2}\left[\frac{1}{(p_- + i\epsilon)^2} + \frac{1}{(p_- - i\epsilon)^2}\right]. \tag{10.5}$$

The dressed quark propagator and the quark self-energy, given in terms of the diagrams in Fig. 10.2, obey the coupled equations,

$$S(p) = \frac{ip_-}{2p_+p_- - m^2 - p_-\Sigma(p) + i\epsilon}$$

$$\Sigma(p) = 4g^2 \int \frac{dk_+ dk_-}{(2\pi)^2} S(p-k)\mathcal{P}\left(\frac{1}{(k_-)^2}\right), \tag{10.6}$$

https://doi.org/10.1017/9781009401654.011 Published online by Cambridge University Press

where Σ is the γ_+ part, the only part that appears in the self-energy in our gauge. If we shift the integration variables $p_+ - k_+ \to -k_+$ we eliminate the dependence on p_+. Hence Σ is only a function of p_-. Due to its Lorentz structure it implies that Σ must be a constant times $\frac{1}{p_-}$, namely $m^2 + p_-\Sigma \equiv M^2$. Thus in the leading large N the sole effect of the interaction, for the propagator, is to replace the quark mass m by a renormalized quark mass M.

Integrating over k_+ we get,

$$\Sigma = \frac{g^2}{2\pi}\int \mathrm{d}k_- \mathrm{sgn}(p_- - k_-)\mathcal{P}\left(\frac{1}{(k_-)^2}\right) = -\frac{g^2}{\pi p_-}, \tag{10.7}$$

and hence,

$$M^2 = m^2 - \frac{g^2}{\pi}. \tag{10.8}$$

In the original treatment of 't Hooft, the regularization employed was not of principal value, but rather of a sharp cutoff, namely integrating over $|p_-| > \lambda$. This avoids the infrared divergence as well, but introduces a new scale, which is not gauge invariant. Obviously, one has to check that Green's functions of gauge invariant operators are independent of λ when $\lambda \to 0$. Thus we find that,

$$\Sigma(p) = \Sigma(p_-) = -\frac{g^2}{\pi}\left(\frac{\mathrm{sgn}(p)}{\lambda} - \frac{1}{p_-}\right), \tag{10.9}$$

and correspondingly the dressed quark propagator is,

$$S(p) = \frac{ip_-}{2p_+p_- - m^2 + \frac{g^2}{\pi} - \frac{g^2|p_-|}{\pi\lambda} + i\epsilon}. \tag{10.10}$$

Now the pole of the quark propagator is shifted towards $k_+ \to \infty$ and hence there is no physical single quark state.

Let us consider now the spectrum of the mesonic bound states. The propagator of the meson is given by the sum of diagrams as is shown in Fig. 10.3.

This ladder sum is exact in the planar limit that follows from the large N approximation. If the propagator has a meson pole, then the ladder diagrams have to obey the Bethe–Salpeter equation as in Fig. 10.4.

The "blob" is the Fourier transform of the matrix element,

$$\tilde{\phi}(p,q) = F.t. <\mathrm{meson}|T\bar{\psi}(x)\psi(0)|0>,$$

with external legs of a quark of mass m, momentum p, and an anti-quark of mass m and momentum $p - q$ (for simplicity, we take one flavor, and so the same mass for the quark and anti-quark). The Bethe–Salpeter equation reads,

$$\tilde{\phi}(p,q) = -4ig^2 S(p-q)S(p)\int \frac{\mathrm{d}^2k}{(2\pi)^2}\mathcal{P}\left(\frac{1}{(k_- - p_-)^2}\right)\tilde{\phi}(k_-,q). \tag{10.11}$$

Defining

$$\phi(p_-,q) = \int \mathrm{d}p_+\tilde{\phi}(p,q),$$

https://doi.org/10.1017/9781009401654.011 Published online by Cambridge University Press

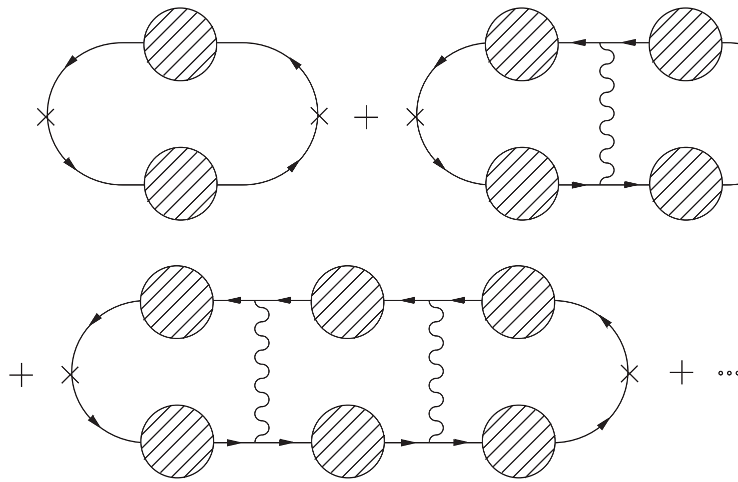

Fig. 10.3. The Green's function of the quark bilinear.

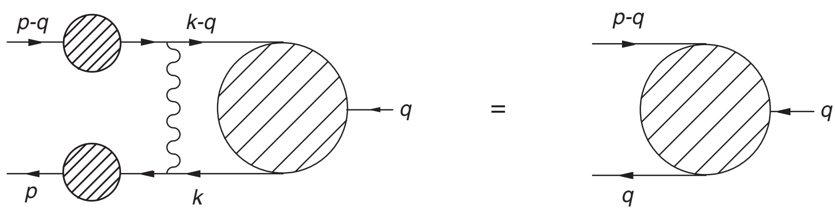

Fig. 10.4. The Bethe–Salpeter equation.

we get,

$$\phi(p_-, q) = -i\frac{g^2}{\pi^2}\int \mathrm{d}p_+ S(p-q)S(p)\int \mathrm{d}k_- \mathcal{P}\left(\frac{1}{(k_- - p_-)^2}\right)\phi(k_-, q). \quad (10.12)$$

The integral over p_+ can be done explicitly

$$\begin{aligned} I(p_-, q) &\equiv \int \mathrm{d}p_+ S(p-q)S(p) \\ &= -\int \mathrm{d}p_+ \frac{1}{\left[2(p_+ - q_+) - \frac{M^2 - i\epsilon}{p_- - q_-}\right]}\frac{1}{\left[2p_+ - \frac{M^2 - i\epsilon}{p_-}\right]}. \end{aligned} \quad (10.13)$$

If p_- is outside the interval $[0, q_-]$ then the two poles are on same side of the real axis, and the integral vanishes. When p_- is inside the interval, the integral is (taking $q_- > 0$),

$$-i\pi\left[2q_+ - \frac{M^2}{p_-} - \frac{M^2}{(q_- - p_-)}\right],$$

so that,

$$\left[2q_+ - \frac{M^2}{p_-} - \frac{M^2}{q_- - p_-)}\right]\phi(p_-, q) = -\frac{g^2}{\pi}\int_0^{q_-} \mathrm{d}k_- \mathcal{P}\left(\frac{1}{(k_- - p_-)^2}\right)\phi(k_-, q). \quad (10.14)$$

https://doi.org/10.1017/9781009401654.011 Published online by Cambridge University Press

Defining x and y by,

$$p_- = xq_-, \quad k_- = yq_-,$$

and,

$$2q_+q_- = \mu^2,$$

one finally gets ’t Hooft’s equation,

$$\mu^2\phi(x) = \left[\frac{M^2}{x} + \frac{M^2}{1-x}\right]\phi(x) - \frac{g^2}{\pi}\int_0^1 \mathrm{d}y \frac{1}{(x-y)^2})\phi(y), \tag{10.15}$$

with $\phi(x)$ defined on the interval $[0,1]$.

The equation cannot be solved analytically, but one can compute the wave-functions that correspond to the various states numerically.

Before describing these solutions let us further discuss the equation. In fact one can derive the equation using a light-cone Schrödinger equation. In the light-cone coordinates a system is specified at x^+, and its dynamics is generated by P_+, the generator of translations of x^+. Since the latter commutes with P_-, the generator of translations of x^-, it is useful to use the eigenspace of P_-. For example, for a free single particle of mass M, $2P_+ = \frac{M^2}{P_-}$. Note however that unlike the ordinary Schrödinger formulation which is expressed in terms of a real line, the spectrum of P_1, in the light-cone case the spectrum of P_- is the positive half-line. For a system of two particles one can always choose to normalize the eigenvalue of P_- to be one, so that the eigenvalue of the operator on one of the two particles is x and the on the other it is $1-x$, such that for two non-interacting particles $2P_+ = \frac{M^2}{x} + \frac{M^2}{1-x}$. This yields the first two terms in (10.15). The other term, the integral, is just a linear potential term. If we interpret temporarily x as a position operator, then the operator form of (10.15) is,

$$2P_+ = \frac{M^2}{x} + \frac{M^2}{1-x} + g^2|p|. \tag{10.16}$$

This is the Hamiltonian of a massless particle moving in a potential and restricted to a box $[0,1]$. This guarantees that the spectrum is discrete and there is no continuum of two free particles. Moreover we can go further with this interpretation and argue that at least for high-level states the eigenstates are like those of a free particle in a box namely,

$$\phi_n \approx \sin(\pi n x), \quad \mu_n^2 \approx g^2\pi n, \tag{10.17}$$

for $n = 1, 2, \ldots$ These states furnish a linear “Regge trajectory” with no continuum. We will verify shortly that for large n this is indeed the structure of the eigenstates and eigenvalues. Since the renormalized quark mass becomes tachyonic for large coupling constant g (eqn. 10.8) one may wonder whether the mesonic bound states can also be tachyonic. It turns out that this cannot occur.

From (10.15) it follows that,

$$\mu^2 \int_0^1 |\phi(x)|^2 \mathrm{d}x = m^2 \int_0^1 |\phi(x)|^2 \left[\frac{1}{x} + \frac{1}{1-x}\right] \mathrm{d}x + \frac{g^2}{2\pi} \int_0^1 \mathrm{d}x \int_0^1 \mathrm{d}y \frac{|\phi(x)||\phi(y)|}{(x-y)^2}. \tag{10.18}$$

To solve the 't Hooft equation (10.15) we need to specify the boundary conditions.

At $x = 0$ ($x = 1$) the solution may behave like $x^{\pm\beta}$ ($(1-x)^{\pm\beta}$) with,

$$\pi\beta \cot g(\pi\beta) + \frac{\pi M^2}{g^2} = 0. \tag{10.19}$$

Let us define the "Hamiltonian" of the system as the right-hand side of equation (10.15), namely,

$$H\phi(x) \equiv \left[\frac{M^2}{x} + \frac{M^2}{1-x}\right] \phi(x) - \frac{g^2}{\pi} \int_0^1 \mathrm{d}y \mathcal{P}\left(\frac{1}{(x-y)^2}\right) \phi(y). \tag{10.20}$$

This Hamiltonian is Hermitian only when acting on the space of functions that vanish on the boundary, as can be seen from (10.18). Using the latter one can show that ϕ_n with $\phi_n(0) = \phi_n(1) = 0$ constitute a complete orthonormal set,

$$\sum_n \phi_n(x)\phi_n(x') = \delta(x - x')$$
$$\int_0^1 \phi_n^*(x)\phi_m(x)\mathrm{d}x = \delta_{nm}. \tag{10.21}$$

Since the integral in (10.15) gets its main contribution from y close to x and since for a periodic function we have,

$$\mathcal{P}\left(\int_0^1 \frac{\mathrm{e}^{iwy}}{(x-y)^2} \mathrm{d}y\right) \simeq \mathcal{P}\left(\int_{-\infty}^{\infty} \frac{\mathrm{e}^{iwy}}{(x-y)^2} \mathrm{d}y\right) = -\pi|w|\mathrm{e}^{iwx}, \tag{10.22}$$

then the configurations given in (10.17) are a good approximation of the eigenstates of the system. The numerical solutions of eqn. (10.15) are drawn in Fig. 10.5.

In this figure the mass spectrum of mesons is shown for various values of quark mass. In cases when the mass of the quark and anti-quark are not equal, the term $[\frac{M^2}{x} + \frac{M^2}{1-x}]$ in (10.15) is replaced by $[\frac{M_1^2}{x} + \frac{M_2^2}{1-x}]$.

The masses and wavefunctions cannot be determined in general in an analytic form. However in certain limits one can write down approximate expressions. In [52] it was shown that the highly excited states $n \gg 1$, where n is the excitation number have masses given by,

$$(M_{\mathrm{mes}})_n^2 \sim \pi g^2 N \left(n + \frac{3}{4}\right) + (m_{q_1}^2 + m_{q_2}^2) ln(n) + C(m_{q_1}^2) + C(m_{q_1}^2) + \mathcal{O}\left(\frac{1}{n}\right), \tag{10.23}$$

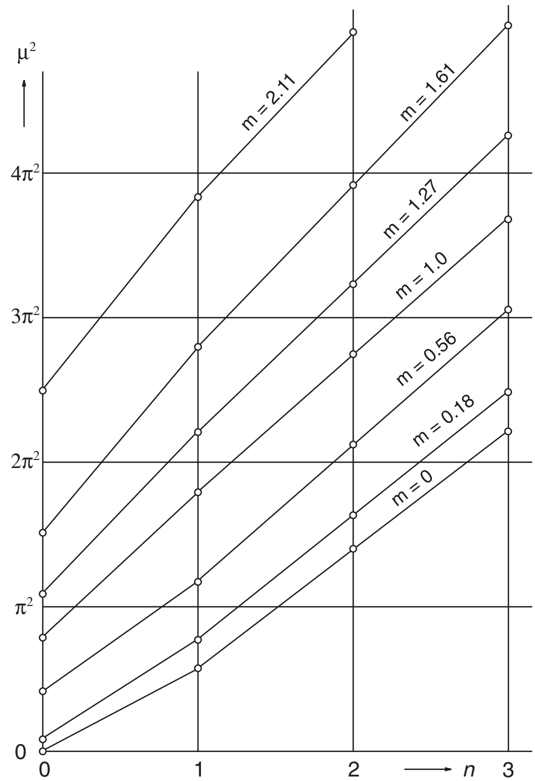

Fig. 10.5. The spectrum of mesons. The squared masses are in units of $\frac{g^2}{\pi}$ [124].

where m_{q_i} are the masses of the quark and anti-quark and where the functions $C(m_q^2)$ are given in [52].

The opposite limit of low-lying states and in particular the ground state can be deduced in the limit of large quark masses, namely $m_q \gg g$ and small quark masses $g \gg m_q$. For the ground state in the former limit one finds,

$$M^0_{\text{mes}} \cong m_{q_1} + m_{q_2}\,. \tag{10.24}$$

In the opposite limit of $m_q \ll g$,

$$(M^0_{\text{mes}})^2 \cong \frac{\pi}{3}\sqrt{\frac{g^2 N_c}{\pi}}(m_1 + m_2). \tag{10.25}$$

For the special case of massless quarks we find a massless meson.

In Fig. 10.6 the spectrum of meson nonets built from two triplets of flavor with masses

$$\begin{aligned} &(a)\ m_1 = 0 \quad m_2 = 0.2 \quad m_3 = 0.4 \\ &(b)\ m_1 = 0.8 \quad m_2 = 1.0 \quad m_3 = 1.2 \end{aligned} \tag{10.26}$$

https://doi.org/10.1017/9781009401654.011 Published online by Cambridge University Press

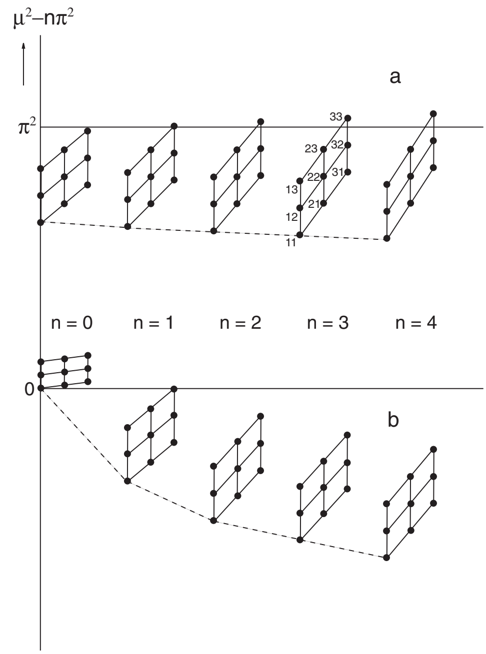

Fig. 10.6. Meson nonets for $N_c = 3$. In case (a) the masses of the triplet are $m_1 = 0.00, m_2 = 0.20, m_3 = 0.4$ and in (b) $m_1 = 0.80, m_2 = 1.00, m_3 = 1.2$ [124].

is shown, in units of $\frac{g}{\sqrt{\pi}}$. Then the ground state is at 2.7, the first excited state at 4.16, and level $n = 10$ is at 20.55. It is obvious from these cases that for larger n, the wavefunction gets more and more sharply picked around $x = 0.5$. For the case of unequal masses, the wavefunction ceases to be symmetric, as can be seen from Fig. 10.7 for $m_1 = 1, m_2 = 5$.

10.1 Scattering of mesons

In the previous section we have described the equation that governs the formation of mesonic bound states, and the corresponding meson spectrum follows from a homogeneous Bethe–Salpeter equation. This can be generalized to the equation for full quark anti-quark scattering amplitude, which takes the form of the non-homogeneous equation of Fig. 10.8.

The scattering amplitude has the following structure,

$$T_{\alpha\beta,\gamma\delta} = (\gamma_-)_{\alpha\gamma}(\gamma_-)_{\beta\delta}T(q, q', p). \tag{10.27}$$

The undressed amplitude $T(q, q', p)$ takes the form,

$$T(q, q', p) = \frac{ig^2}{(q_- - q'_-)^2} + \frac{ig^2 N}{\pi^2}\int \frac{\mathrm{d}k_-\phi(k_-, q', p)}{(k_- - q_-)^2}, \tag{10.28}$$

https://doi.org/10.1017/9781009401654.011 Published online by Cambridge University Press

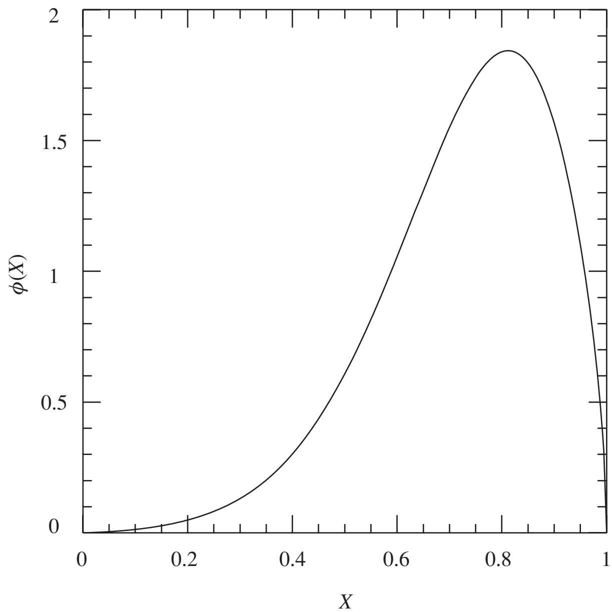

Fig. 10.7. Wavefunction for $m_1 = 1, m_2 = 5$.

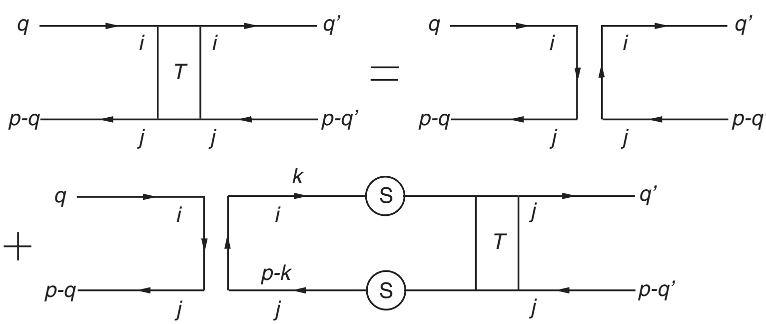

Fig. 10.8. The Bethe–Salpeter equation for quark anti-quark scattering.

where,

$$\phi(q_-, q'_-, p) = \int \mathrm{d}q_+ S_E(q) S_E(q - p) T(q, q', p). \tag{10.29}$$

Similar to the equation for the "wave function" $\phi(x)$ we now get the generalization to $\phi(x, x', p)$ which reads,

$$\mu^2 \phi(x, x', p) = \left[\frac{M^2}{x} + \frac{M^2}{1 - x}\right] \phi(x, x', p) + \frac{\pi^2}{N p_- (x - x')^2} + \int_0^1 \mathrm{d}y \frac{[\phi(x, x', p) - \phi(y, x', p)]}{(x - y)^2}. \tag{10.30}$$

https://doi.org/10.1017/9781009401654.011 Published online by Cambridge University Press

It is now straightforward to express $\phi(x,x',p)$ in terms of $\phi(x)$ as,

$$\phi(x,x',p) = -\sum_n \frac{\pi g^2}{p^2-p_n^2}\frac{1}{p_-}\int_0^1 \mathrm{d}y \frac{\phi_n(x)\phi*_n(y)}{(x-y)^2}, \tag{10.31}$$

and substituting this into (10.28) we find the scattering amplitude,

$$\begin{aligned} T(x,x',p) = {} & \frac{ig^2}{p_-^2(x'-x)^2} - \frac{ig^2(g^2N)}{\pi p_-^2}\sum_n \frac{1}{p^2-p_n^2} \\ & \times \int_0^1 \mathrm{d}y \int_0^1 \mathrm{d}y' \frac{\phi_n(y)\phi*_n(y')}{(x-y)^2(x'-y')^2} = \frac{ig^2}{p_-^2(x'-x)^2} - \sum_n \frac{1}{p^2-p_n^2} \\ & \left[\phi_n^*(x')\frac{2g}{\lambda}\sqrt{\frac{g^2N}{\pi}}\left(\theta(x'(1-x'))+\frac{\lambda}{2|p_-|}\left(\frac{\gamma_1-1}{x'}+\frac{\gamma_2-1}{1-x'}-\mu_k^2\right)\right)\right] \\ & \times [(x'\leftrightarrow x)], \end{aligned} \tag{10.32}$$

where γ_i for $i=1,2$ are $\frac{M_i}{(\frac{g}{\sqrt{\pi}})}$.

This clarifies the dynamics of the confinement. The infinite self-mass quark is cancelled by the quark anti-quark interaction producing finite mass color singlet bound states, whose mass squared, as we have seen above, increases linearly for high excited states. The infrared behavior is determined by the dependence on λ as in (10.9). The bound state wave function is of order $\frac{1}{\lambda}$ as $\lambda \to 0$. The fact that the amplitude for a bound state to decay into quarks is infinite as $\lambda \to 0$ compensates for the vanishing quark propagator in this limit to produce finite bound state amplitudes, which contain no multiquark discontinuities.

To test the consistency of the model one has to examine also the hadronic scattering processes. One has to check that these are finite in the limit of $\lambda \to 0$, unitary and Lorentz invariant. A consequence of the unitarity is the absence of long range forces among the color singlets.

In Fig. 10.9 the three-particle vertex function and the two-particle scattering are drawn. The three-particle vertex function, Fig. 10.9(a), is of order $g \sim \frac{1}{\sqrt{N}}$. Each quark propagator is of order λ. The k_+ loop momentum is of order $\frac{1}{\lambda}$ since it is dominated by the pole at $\frac{1}{\lambda}$. From the three bound state wave functions we get a factor of $(\frac{1}{\lambda})^2$ since at least one wave function must be of order unity to conserve momentum. So altogether the factors of λ cancel out and we get a finite result in the limit of $\lambda \to 0$.

The two-particle scattering is described in Fig. 10.9(b) and 10.9(c). The former describes a hadronic exchange and the latter a quark exchange. The quark exchange may seem to be infinite in the limit $\lambda \to 0$ since now the quark and anti-quark can move in the same direction with an amplitude that behaves like $\frac{1}{\lambda}$. The total dependence on λ is as follows: λ^4 from quark propagators, $\frac{1}{\lambda^4}$ from the wave functions and $\frac{1}{\lambda}$ from the loop momentum integration. However it can be shown that when one adds all diagrams that contribute to $\frac{1}{N}$ order, the terms of

https://doi.org/10.1017/9781009401654.011 Published online by Cambridge University Press

(a)

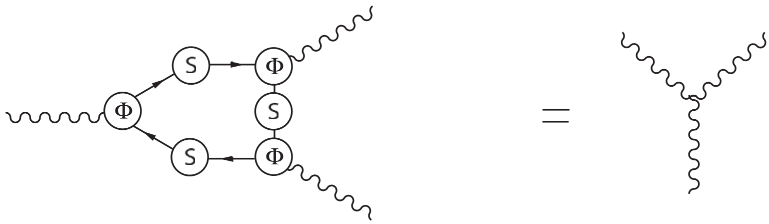

(b)

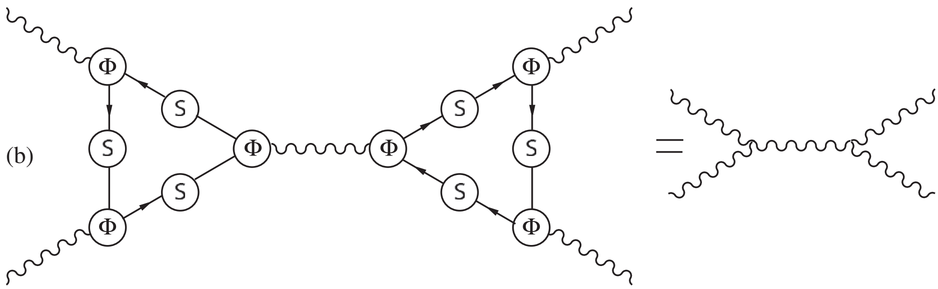

(c)

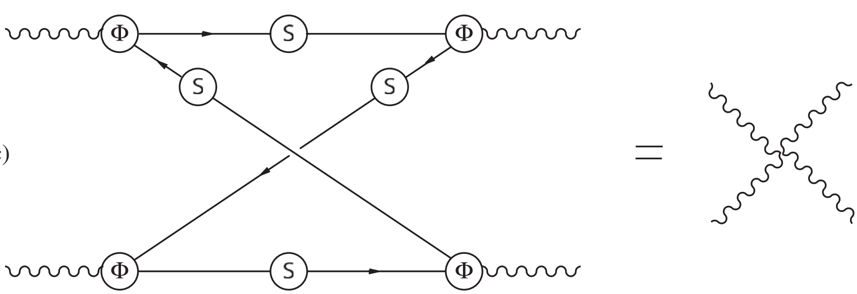

Fig. 10.9. (a) Three-particle vertex function. (b) Hadronic exchange contribution to two-particle scattering amplitude. (c) Quark exchange contribution to two-particle scattering amplitude.

order $\frac{1}{\lambda}$ cancel, leaving a finite remainder. In this way we have verified unitarity of the model to the first non-trivial order.

10.2 Higher $1/N$ corrections

At $N = \infty$ the mesons are stable since their decay rate, as will be shown shortly, is proportional to $\frac{1}{N}$. Going to the $\frac{1}{N}$ corrections, a meson has the following amplitude to decay into two mesons[1]

$$\mathcal{A}(i, f_1, f_2; w) = \frac{4g^2\sqrt{N}}{\sqrt{\pi}} \left\{ \frac{1}{1-w} \int_0^w \mathrm{d}x \phi_i(x) \phi_{f_1}\left(\frac{x}{w}\right) \Phi_{f_2}\left(\frac{x-w}{1-w}\right) \right.$$
$$\left. - \frac{1}{w} \int_w^1 \mathrm{d}x \phi_i(x) \Phi_{f_1}\left(\frac{x}{w}\right) \phi_{f_2}\left(\frac{x-w}{1-w}\right) \right\}, \qquad (10.33)$$

[1] The $1/N$ corrections were evaluated in [144].

https://doi.org/10.1017/9781009401654.011 Published online by Cambridge University Press

where $\phi_i, \phi_{f_1}, \phi_{f_2}$ are the wave functions of the initial meson and first and second final mesons, respectively. The quark ends up being in the second final meson and the anti-quark in the first final meson. The vertex function $\Phi(x)$, with x *not* $\in [0,1]$, is related to the wave function as,

$$\Phi(x) = \int_0^1 \mathrm{d}y \frac{1}{(x-y)^2}\phi(y). \tag{10.34}$$

The kinematic parameter w takes the values,

$$w_\pm = \frac{\mu_i^2 + \mu_{f_1}^2 - \mu_{f_2}^2 \mp \sqrt{(\mu_i^2 + \mu_{f_1}^2 - \mu_{f_2}^2)^2 - 4\mu_i^2\mu_{f_2}^2}}{2\mu_i^2}, \tag{10.35}$$

where w_+ and w_- correspond to the right and left moving final state f_1. The decay can take place only provided $\mu_i \geq \mu_{f_1} + \mu_{f_2}$. It is clear that for fixed g^2N the amplitude is of order $\mathcal{A} \sim O(\frac{1}{\sqrt{N}})$. The amplitude (10.33) is for a partial decay and for full-on shell amplitude one has to add the partial decays

$$\mathcal{A} = (1 - (-1)^{\sigma_i + \sigma_{f_1} + \sigma_{f_2}})(\mathcal{A}(i, f_1, f_2; w_+) + \mathcal{A}(i, f_1, f_2; w_-)), \tag{10.36}$$

with σ_+ for even parity state and σ_- for odd parity state. It was found that numerically these amplitudes for various excited states do not vanish. This also shows that the model is *not integrable.*

It was further found that the amplitudes for mesons made out of massless quark anti-quark pairs differ significantly from those of mesons made out of massive ones. An interesting result that follows from the computations of these amplitudes is that the amplitude for decay of an exited meson into a pion and another meson vanishes, in the case of massless quarks. This is actually to be expected, as for massless quarks the two-dimensional pion is massless and decoupled, since there is no chiral symmetry breaking in two dimensions.